PERGAMON

Journal of Structural Geology 24 (2002) 557–565

JOURNAL OF STRUCTURAL GEOLOGY

www.elsevier.com/locate/jstrugeo

Lattice preferred orientation of quartz inclusions within garnet porphyroblasts from the Imjingang belt, South Korea

W.-S. Jung[a], J.-H. Ree[a,*], Y. Park[a], S.-H. Choi[b]

[a]*Department of Earth and Environmental Sciences, Korea University, Seoul 136-701, South Korea*
[b]*Department of Earth and Environmental Sciences, Chungbuk National University, Chongju 361-763, South Korea*

Received 22 March 2000; revised 11 June 2001; accepted 19 June 2001

Abstract

Quartz inclusions within intertectonic garnet porphyroblasts of metapelites from the southern Imjingang belt have a lattice preferred orientation. *c*-Axis fabrics of the quartz inclusions tend to show a single girdle pattern at a high angle to an earlier foliation together with a submaximum subparallel to an earlier lineation. This lattice preferred orientation of the quartz inclusions might result from intracrystalline deformation together with solution creep prior to the garnet growth or from selective entrapment of quartz grains with a specific lattice orientation during the garnet growth.

Keywords: Garnet porphyroblast; Quartz inclusions; *c*-Axis fabric; Imjingang belt

1. Introduction

Inclusions within rigid porphyroblasts can be protected during a deformation later than or concurrent with the porphyroblast growth. If porphyroblasts statically grown between two deformation events (i.e. *intertectonic* porphyroblast of Passchier and Trouw (1996)) do not rotate during later deformation or if we know the rotation amount of intertectonic porphyroblasts, the inclusions within porphyroblasts may provide some information on the earlier deformation. For example, the attitude of earlier foliation can be obtained using straight inclusion trails within intertectonic porphyroblasts (Steinhardt, 1989; Jung et al., 1999). Also, the attitude of earlier fold axis can be measured by analyzing the geometry of inclusion trails within porphyroblasts (Hayward, 1990; Johnson, 1993; Bell and Hickey, 1997). Furthermore, if we know the orientation of earlier foliation and lineation, the kinematics and characteristics of earlier deformation may be inferred using *c*-axis fabrics of quartz inclusions within intertectonic porphyroblasts.

c-Axis fabrics of quartz inclusions have rarely been used to interpret the kinematics of deformation earlier than the growth of porphyroblasts, although Vissers (1989) measured *c*-axis orientation of quartz inclusions within porphyroblasts to confirm the initially random orientation of *c*-axis prior to the growth of the porphyroblasts. This study presents *c*-axis fabrics of quartz inclusions within intertectonic garnet porphyroblasts and discusses the kinematics and microstructural processes of an earlier deformation. The analyzed samples are from the Imjingang orogenic belt of the central Korean peninsula.

2. Geological framework

The Yeoncheon complex occurs in the southern Imjingang orogenic belt in the central Korean peninsula (Fig. 1). Hsü et al. (1990) and Ree et al. (1996) suggested that the Imjingang belt is an eastward extension of Qinling–Dabie–Sulu collisional belt of east-central China. The Yeoncheon complex is divided into two main rock units (Ree et al., 1996). The Late Proterozoic Samgot unit in the south consists of calc–silicate and amphibolite with minor metapelite and metapsammite. The Silurian–Devonian Jingok unit in the north is composed of pelitic to semipelitic schist, phyllite, and quartzite with minor marble. The boundary between the Samgot and Jingok units is characterized by a normal fault developed during post-collisional uplift (Fig. 1).

Metapelites of the Jingok unit can be grouped into three zones with a typical Barrovian paragenetic sequence, increasing in grade southward (garnet → staurolite → kyanite zone) (Fig. 1b). The occurrences of garnet, garnet + staurolite, and garnet + staurolite + kyanite, respectively,

* Corresponding author. Tel.: +82-2-3290-3175; fax: +82-2-3290-3189.
E-mail address: reejh@korea.ac.kr (J.-H. Ree).

0191-8141/02/$ - see front matter
PII: S0191-8141(01)00083-9

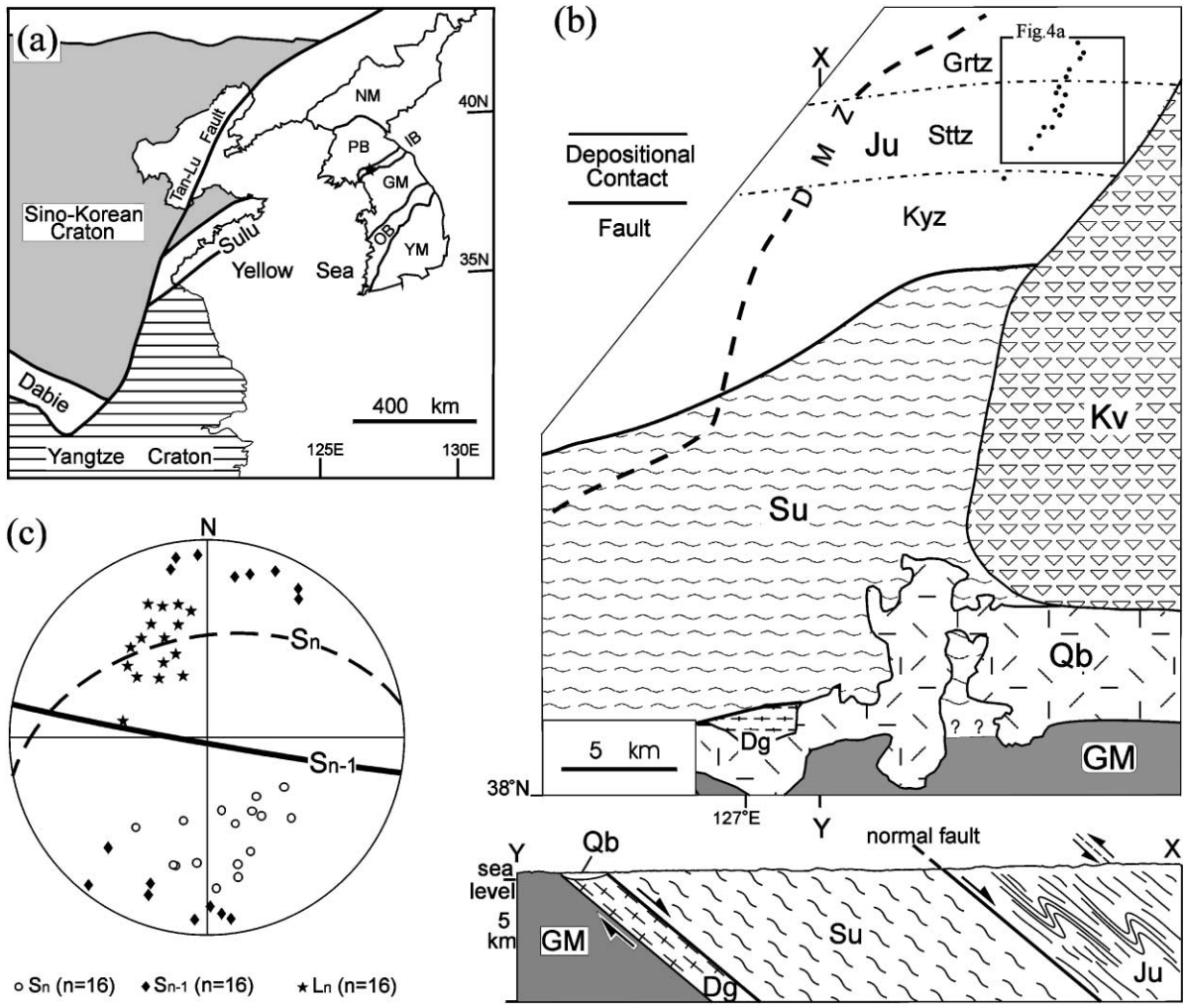

Fig. 1. (a) Simplified geologic map of northeast Asia. NM = Nangrim massif, PB = Pyeongnam basin, IB = Imjingang belt, GM = Gyeonggi massif, OB = Ogcheon belt, YM = Yeongnam massif. The Yeoncheon area of (b) is represented by a star. (b) Geologic map and schematic cross-section of Yeoncheon area (after Ree et al., 1996): Ju = Jingok unit, Grtz = garnet zone, Sttz = staurolite zone, Kyz = kyanite zone, Su = Samgot unit, Dg = deformed granitoid, GM = Gyeonggi massif gneiss, Kv = Cretaceous (?) tuff, Qb = Quaternary basalt, DMZ = southern boundary of the Demilitarized Zone. Solid dots represent the outcrops where the attitude of S_{n-1} was measured using inclusion trails within garnet porphyroblasts. (c) Stereogram of lineation (L_n), and poles to S_n and S_{n-1}. Great circles represent mean S_n and S_{n-1}. Lower-hemisphere, equal-area projection.

are characteristics of the three zones (Ree et al., 1996). The penetrative foliation (S_n) generally strikes east to northeast and dips consistently north at 40–50° (Fig. 1c). The foliation shows a strong down-dip mineral/elongation lineation that plunges north-northwest at 30–50°. The common occurrence of intrafolial folds of quartz-rich layers in an apparently simply foliated matrix on sections normal to the foliation and parallel to the lineation suggests an intense transposition. All sense of shear indicators including south vergent, tight to isoclinal mesoscopic folds, asymmetric strain shadows around porphyroblasts, and shear bands indicate a top-up-to-the-south (reverse) shear sense (Fig. 2). These structures are interpreted to have developed by contractional deformation, probably during the Permian–Triassic collision between the Sino–Korean and Yangtze cratons (Ree et al., 1996).

3. *c*-Axis fabric of quartz inclusions

3.1. Garnet porphyroblast

The garnet porphyroblasts in the Jingok unit are equidimensional with a diameter of 1–2 mm. Most of the garnet porphyroblasts have straight inclusion trails oblique to an external foliation ($S_e = S_n$, formed during D_n deformation event) on planes normal to mineral/elongation lineation (A_{D_n} plane, facing south), and planes normal to the foliation and parallel to the lineation (B_{D_n} plane, facing east) (Figs. 2a and 3a). These inclusions are mostly quartz and some plagioclase with minor opaque grains. Quartz inclusions occur as single grain or polycrystalline aggregates. The quartz inclusions are equidimensional or elongated in the B_{D_n} plane with their arrangement defining straight inclusion

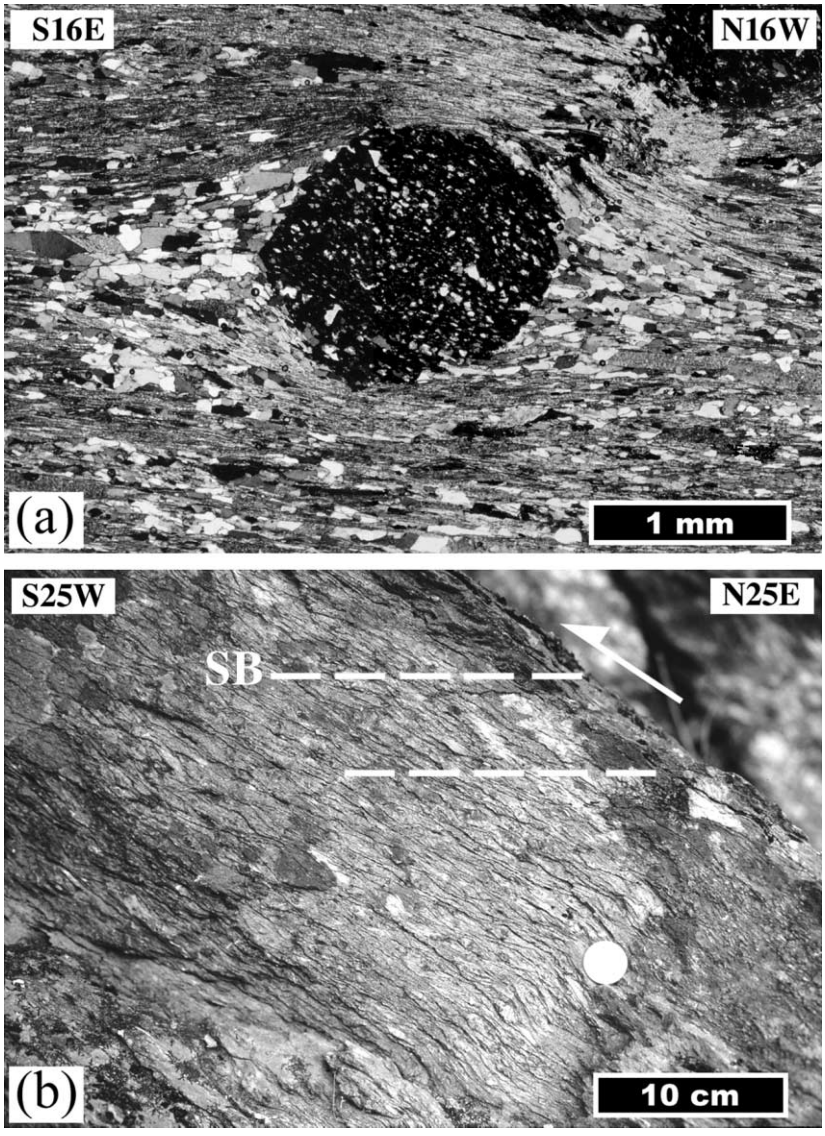

Fig. 2. (a) Photomicrograph of asymmetric strain shadow around garnet porphyroblast indicating top-up-to-the-south shear sense in the plane perpendicular to foliation (S_n) and parallel to lineation (L_n). Note the continuity between the inclusion trails (S_i) and external foliation (S_n). Cross-polarized light. (b) Outcrop photo of shear band indicating top-up-to-the-south shear sense. The outcrop face is roughly parallel to lineation (L_n) and normal to foliation (S_n).

trails (S_i) (Fig. 2a). The size of quartz inclusions is variable (20–125 μm) in each garnet and smaller than that of quartz grains in the matrix (70–250 μm). Plagioclase inclusions are transparent without twinning and were distinguished from quartz inclusions using cathodoluminescence microscopy or electron microprobe analyses. Mostly internal foliation defined by inclusion trails (S_i) and external foliation (S_e) are continuous (Fig. 2a), but in some cases their continuity is not clear due to replacement of garnet rims by chlorite.

Jung et al. (1999) have identified by serial polishing and reflected-light microscopy that the inclusion trails within garnet porphyroblasts are a planar structure (internal foliation: S_i). They have also interpreted that the garnet porphyroblasts grew after the formation of the earlier foliation (remained as S_i or S_{n-1} formed during D_{n-1} deformation event), but before the formation of S_n ($= S_e$) or reorientation of S_{n-1}. They are therefore intertectonic porphyroblasts. Measurement of angles between S_i and S_e on two perpendicular planes (planes A_{D_n} and B_{D_n}) from samples of sixteen outcrops shows that S_i orientation of individual garnets is constant (with 5–30° variation) in each sample (Jung et al., 1999). The attitude of S_i in the geographic space (see Fig. 1c), determined by using its pitch angles on planes A_{D_n} and B_{D_n}, is more or less constant throughout the area (the value of 95% cone of confidence = 10.2°; see Jung et al., 1999). Jung et al. (1999) suggested that these intertectonic garnet porphyroblasts did not rotate with respect to the geographic reference frame during D_n deformation, mainly based on the inconsistency of shear sense inferred from the 'classical' S_i/S_e relationship (assuming garnet rotation) with that inferred

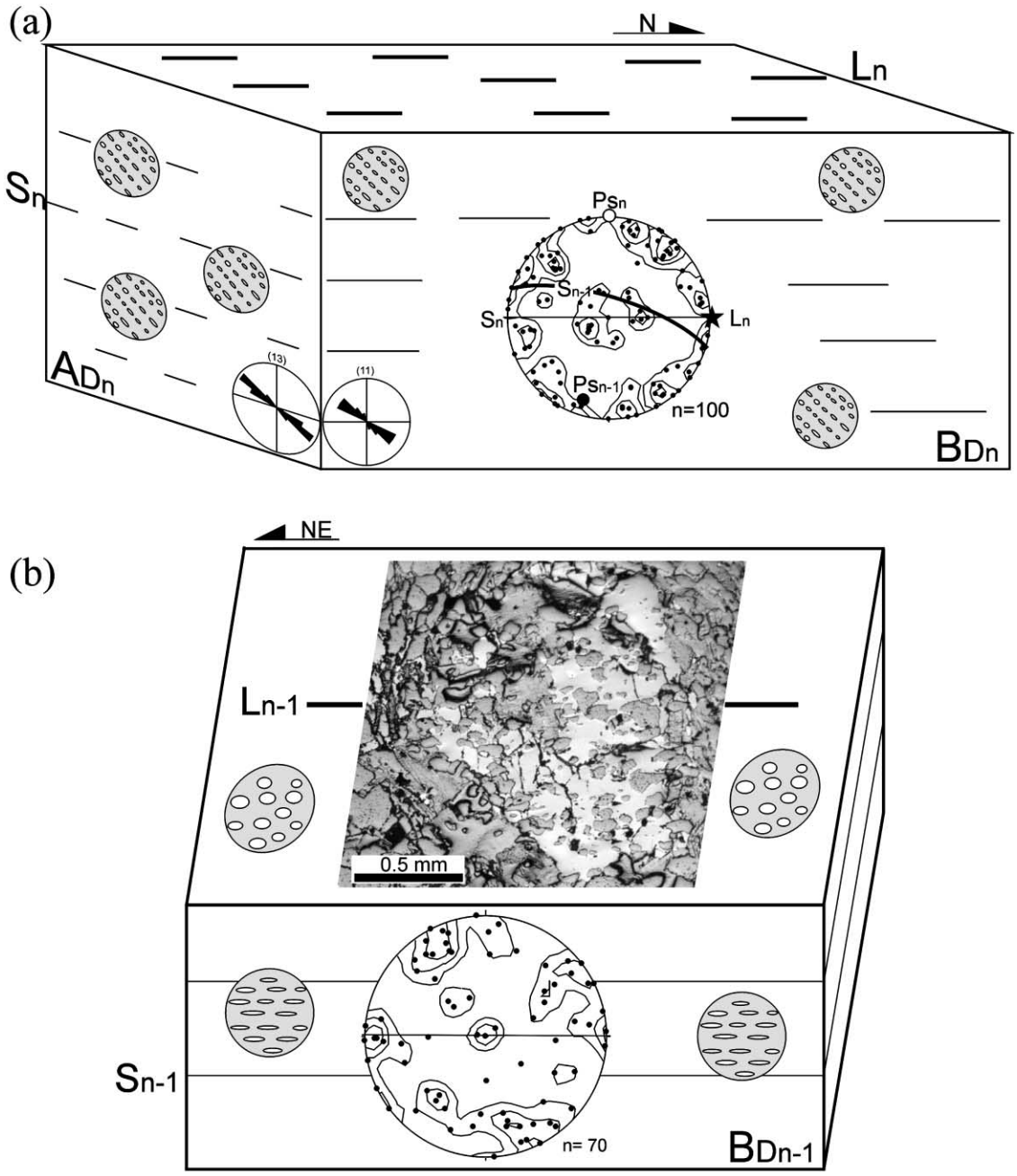
(a)
N
Ln
Sn
ADn
(13)
(11)
PSn
Sn-1
Sn
Ln
PSn-1
n=100
BDn
(b)
NE
Ln-1
0.5 mm
Sn-1
n= 70
BDn-1
(c)
original data
first rotated data
second rotated data
PSn
Sn-1
Sn
Ln
PSn-1
n=100
PSn-1
Sn-1
PSn-1
Sn-1
Ln-1
(Ln-1:S82W/53, R=120)

from all other shear sense indicators (Fig. 2) and constant orientation of earlier foliation defined by inclusion trails. If so, the orientation of planar S_i within the garnet porphyroblasts represents the attitude of the earlier foliation (S_{n-1}) developed during the earlier deformation (D_{n-1}).

Most quartz inclusions are optically strain-free, but some show evidence of plastic deformation (e.g. undulose extinction and subgrains). Most boundaries between quartz grains of inclusions are straight, although lobate boundaries indicating grain boundary migration occasionally occur.

3.2. Measurement of c-axis of quartz inclusions on $B_{D_{n-1}}$ plane

Four samples from two outcrops (YC083 from garnet zone and YC045 from staurolite zone) of the Jingok unit were prepared for measuring the *c*-axis orientations of quartz inclusions within garnet porphyroblasts using a universal stage. Thin sections for measuring the *c*-axis of quartz inclusions were made in the plane normal to S_{n-1} and parallel to L_{n-1} ($B_{D_{n-1}}$ plane). The attitude of S_{n-1} ($=S_i$) was determined by using its pitch angles on two mutually perpendicular planes normal to S_n, as mentioned earlier. The reflected light photomicrograph (Fig. 3b) shows inclusion shapes on S_{n-1} plane less elongated than the inclusion shapes observed on A_{D_n} and B_{D_n} planes (Fig. 2a). This confirms that our method determining S_{n-1} plane using the pitch angles is reasonable. The earlier lineation (L_{n-1}) is defined by a preferred orientation of elongated quartz inclusions on planes parallel to S_{n-1} (see photo of Fig. 3b). The orientation of this L_{n-1} measured on S_{n-1} plane is more or less constant through the area with the average trend and plunge of S70°W and 50°, respectively (see Fig. 4b).

The *c*-axis fabric measured on the $B_{D_{n-1}}$ plane tends to show a single girdle pattern at a high angle to S_{n-1} (stereograms of (1) and (2) of outcrops of YC083 and YC045 in Fig. 4). Also, a sub-maximum of *c*-axis tends to occur subparallel to L_{n-1} (flow direction of D_{n-1}), particularly for sample YC045.

3.3. c-Axis fabric on B_{D_n} plane

Interpretation of *c*-axis fabric of quartz inclusions on $B_{D_{n-1}}$ plane is also possible with the *c*-axis fabric data of quartz inclusions measured on the B_{D_n} plane, if an appropriate rotation of *c*-axis data is applied. Three thin sections (YC083 from garnet zone, and YC302 and YC045 from staurolite zone) of the Jingok unit, cut parallel to plane B_{D_n} (prepared for kinematic studies of D_n), were used for measuring the *c*-axis of quartz inclusions within garnet porphyroblasts.

To make a kinematic interpretation of D_{n-1}, a method similar to that of MacCready (1996) was employed. Fig. 3c illustrates the method using the *c*-axis data of quartz inclusions within a garnet porphyroblast from outcrop YC045. The left stereogram shows the *c*-axis data of quartz inclusions within a garnet porphyroblast measured in a thin section parallel to plane B_{D_n} (see Fig. 3a). *c*-Axis fabric of quartz inclusions show a preferred orientation with a clustering on the primitive circle of the stereogram. The central stereogram shows the first rotated result so that S_{n-1} becomes the equatorial great circle of stereogram, using STEREOPLOT version 3 (Mancktelow, 1995). This was subsequently rotated clockwise at various amounts with the rotation axis being the pole to S_{n-1}. The right stereogram shows the most reasonable pattern in which the *c*-axis girdle is at a high angle to S_{n-1} with a sub-maximum sub-perpendicular to the girdle. L_{n-1} can be inferred to be at 90° from the center of the stereogram along the S_{n-1} plane when rotated *c*-axis data show a reasonable fabric pattern comparable with typical published ones with the assumption of monoclinic flow (e.g. Lister and Hobbs, 1980; Schmid and Casey, 1986; Law, 1990; MacCready, 1996) and also to the *c*-axis pattern directly measured on $B_{D_{n-1}}$ as described earlier. Thus, the trend and plunge of the L_{n-1} inferred from the rotation of *c*-axis data in this sample are S82°W and 53°, respectively.

Fig. 4 shows rotated quartz *c*-axis data within seven garnet porphyroblasts from three outcrops (stereograms (3) and (4) of YC083, (1) and (2) of YC302, and (3), (4), and (5) of YC045). After the rotation steps mentioned earlier, all samples show a single girdle pattern of *c*-axes. *c*-Axis fabrics from outcrops YC302 and YC045 tend to show a sub-maximum at a high angle to the girdle (or subparallel to inferred L_{n-1}). The inferred earlier lineation (L_{n-1}) is subparallel not only to each other but also to L_{n-1} directly measured on S_{n-1} plane with its average trend and plunge of S78°W and 48°, respectively (Fig. 4b). *c*-Axis fabric obtained from this method is also similar to that directly measured on $B_{D_{n-1}}$ plane (Fig. 4a).

4. Discussion

The quartz inclusions within intertectonic garnet porphyroblasts in the Jingok unit tend to display a single-girdle *c*-axis

Fig. 3. (a) Rose diagrams of S_{n-1} orientation of sample YC045 on planes A_{D_n} and B_{D_n} with S_n ($=S_e$) as the horizontal reference line. The number on top of the rose diagram indicates number of garnet porphyroblasts measured. Schematic diagram of garnets with straight inclusion trails is shown on planes A_{D_n} and B_{D_n}. *c*-Axis fabric of quartz inclusions within a garnet porphyroblast measured on B_{D_n} plane is also shown. P_{S_n}: pole to S_n. $P_{S_{n-1}}$: pole to S_{n-1}. (b) *c*-Axis fabric of quartz inclusions within garnet porphyroblast measured on $B_{D_{n-1}}$ plane and photomicrograph showing L_{n-1} defined by preferred orientation of elongated quartz inclusions within garnet on S_{n-1} plane. Contours 1, 2 and 3% per 1% area. Lower-hemisphere, equal-area projection. Schematic shapes of quartz inclusions within garnet are shown on S_{n-1} plane and $B_{D_{n-1}}$ plane. (c) Left: *c*-axis fabric of quartz inclusions as in (b). Center: *c*-axis fabric after rotation so that S_{n-1} becomes the equatorial great circle of stereogram. Right: *c*-axis fabric after further rotation with the pole to S_{n-1} as the rotation axis until the *c*-axis girdle becomes at a high angle to S_{n-1}. *R*: rotation angle. See text for details.

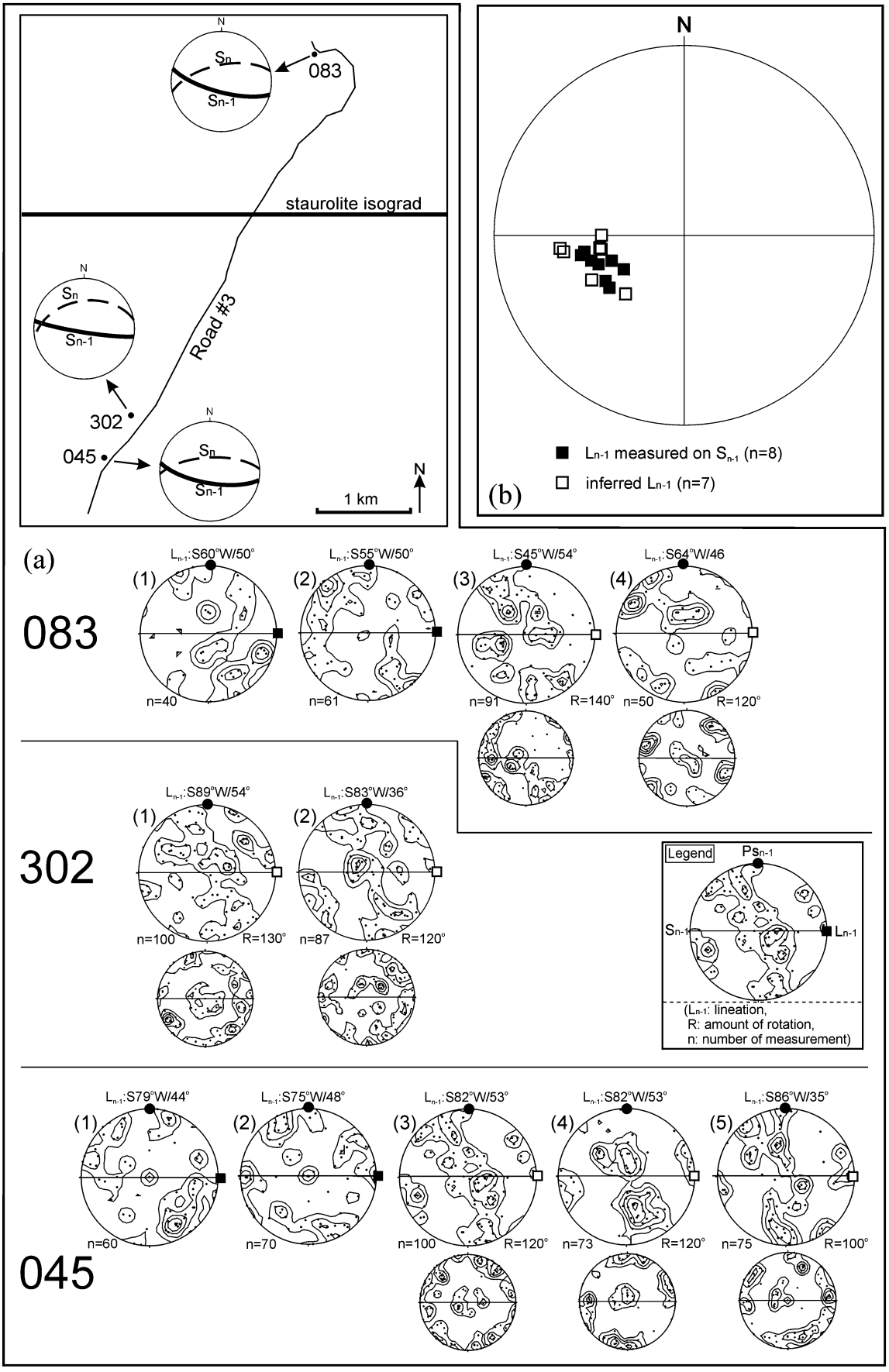
(a)
N
Sn
Sn-1
083
staurolite isograd
Road #3
302
045
1 km
(b)
Ln-1 measured on Sn-1 (n=8)
inferred Ln-1 (n=7)
083
Ln-1:S60°W/50°
n=40
Ln-1:S55°W/50°
n=61
Ln-1:S45°W/54°
n=91
R=140°
Ln-1:S64°W/46
n=50
R=120°
302
Ln-1:S89°W/54°
n=100
R=130°
Ln-1:S83°W/36°
n=87
R=120°
Legend
Psn-1
Sn-1
Ln-1
(Ln-1: lineation,
R: amount of rotation,
n: number of measurement)
045
Ln-1:S79°W/44°
n=60
Ln-1:S75°W/48°
n=70
Ln-1:S82°W/53°
n=100
R=120°
Ln-1:S82°W/53°
n=73
R=120°
Ln-1:S86°W/35°
n=75
R=100°

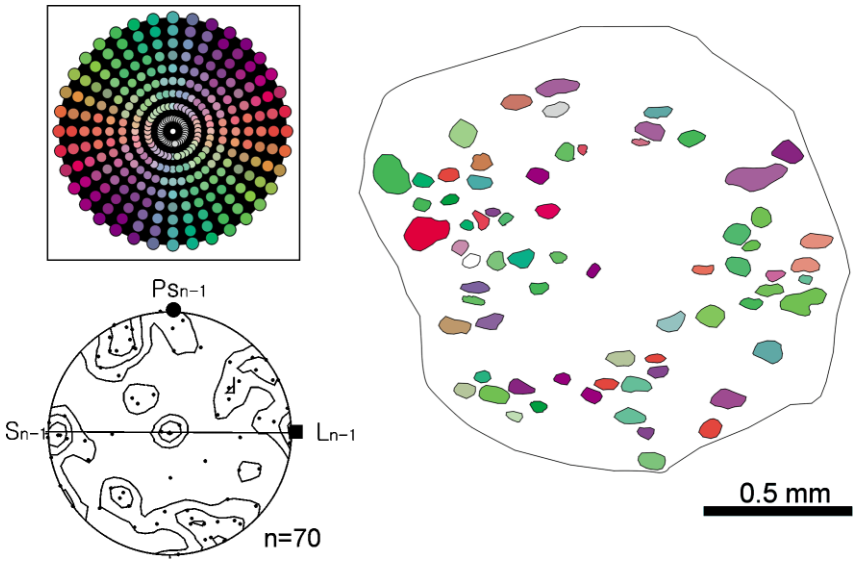

Fig. 5. AVA diagram and *c*-axis fabric of quartz inclusions within a garnet porphyroblast on $B_{D_{n-1}}$ plane. Color chart in the box is the reference for the *c*-axis orientation. Contours 1, 2 and 3% per 1% area. Lower-hemisphere, equal-area projection.

fabric together with a sub-maximum of *c*-axis subparallel to an earlier lineation (L_{n-1}). The single-girdle pattern of *c*-axis fabric can be interpreted as resulting from intracrystalline deformation under a bulk non-coaxial flow regime with the operation of basal, prism and rhomb slip systems (Schmid and Casey, 1986; Knipe and Law, 1987; Law, 1990). Also, the reliable movement sense of the earlier deformation can be inferred from the obliquity of the *c*-axis girdle with respect to the earlier foliation, assuming a monoclinic flow. The obliquity of the *c*-axis girdles consistently indicates a top-up-to-the-NE movement sense for the earlier deformation (sinistral in Figs. 3b and 4a). Of course, the *c*-axis fabric clustering on the primitive circle (i.e. *c*-axis pattern before our two stages of rotation or measured in the B_{D_n} plane) can be formed on the vorticity profile plane in an X_I-shear zone (Passchier, 1998) or in a triclinic shear zone (Jiang and Williams, 1998). Structural evidence to determine the flow type of D_{n-1} deformation is scarce due to the intense D_n deformation in the study area, although the earlier structural elements have been reported to be better preserved in the less deformed area of the North Korean side of the Imjingang belt (Yamaguchi, 1951).

The sub-maximum of quartz *c*-axis that lies close to the earlier lineation can be attributed to; (1) operation of prism ⟨c⟩ slip, (2) entrapment of quartz grains growing in strain shadow areas with their *c*-axis parallel to the extension direction, (3) inheritance from originally elongated detrital quartz grains with their longer dimension parallel to the *c*-axis, (4) selective entrapment of quartz grains with a specific crystallographic orientation during the garnet growth, and (5) entrapment of quartz grains most resistant to dissolution and possibly grains grown with *c*-axis parallel to elongation direction via solution transfer. We discuss these possibilities below.

A *c*-axis fabric parallel to the elongation lineation has commonly been interpreted to indicate the operation of prism ⟨c⟩ slip (e.g. Mainprice et al., 1986). The activation of prism ⟨c⟩ slip system requires a high temperature usually under upper amphibolite or granulite facies condition (e.g. Behr, 1980; Lister and Dornsiepen, 1982; Blumenfeld et al., 1986; Mainprice et al., 1986), although Garbutt and Teyssier (1991) reported the operation of prism ⟨c⟩ slip under epidote–amphibolite facies condition with a circulation of hot fluids. However, there is no evidence of such a high metamorphic condition in the study area prior to the Barrovian-type regional metamorphism during which garnet porphyroblasts grew (Yamaguchi, 1951; Ree et al., 1996; Ahn, 1999).

Quartz grains growing in strain shadow and pull-apart areas tend to have their *c*-axis parallel to the extension direction (e.g. Hippertt, 1993; Stallard and Shelley, 1995). If the quartz grains growing in strain shadow areas are successively entrapped in a growing garnet porphyroblast, these quartz grains with their *c*-axis parallel to the extension direction should show a spatial distribution within the garnet porphyroblast. However, there is no such a spatial distribution of quartz grains with a specific *c*-axis orientation within

Fig. 4. (a) *c*-Axis fabric stereograms of quartz inclusions within garnet on $B_{D_{n-1}}$ plane from three outcrops. Stereograms with *R* (rotation) value represent *c*-axis fabrics obtained by the rotation procedure as in Fig. 3(c). Smaller stereograms show *c*-axis fabrics before the rotation procedure. Those without *R* show *c*-axis fabrics directly measured on $B_{D_{n-1}}$ plane. Legend for symbols is shown in box. Contours 1, 2, 3 and 4% per 1% area. (b) Stereogram of measured L_{n-1} (filled square) and inferred L_{n-1} (open square). Lower-hemisphere, equal-area projection.

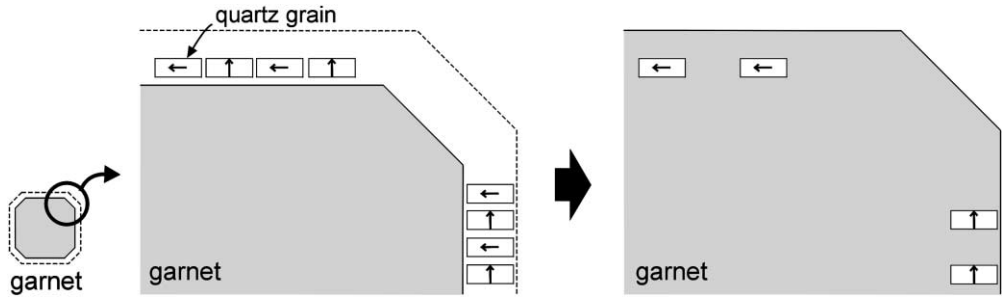

Fig. 6. Schematic diagram illustrating selective entrapment of quartz grains with *c*-axis at a low angle to the migrating phase boundaries between garnet and quartz (see text for details). The arrow in each quartz grain indicates the *c*-axis orientation.

garnet porphyroblasts in the study area, as seen in the AVA diagram of Fig. 5.

It has been suggested that elongated clastic quartz grains preferentially broken parallel to prism faces can have a preferred orientation of *c*-axis due to a mechanical rotation during deposition and compaction (e.g. Bloss and Gibbs, 1963; Stallard and Shelley, 1995). If the extension direction of a subsequent deformation happens to be parallel to the *c*-axis preferred orientation of this sedimentary origin, then the deformed rocks may have a *c*-axis preferred orientation of quartz grains parallel to the elongation lineation. However, this is an unusual case and the original *c*-axis fabric of sedimentary origin can easily be modified during the subsequent plastic deformation unless there is a high-temperature deformation favoring prism ⟨c⟩ slip.

There is a possibility that a garnet porphyroblast selectively entrapped quartz grains with a specific lattice orientation. Fig. 6 schematically illustrates a two-dimensional situation where the selective entrapment occurs due to the preferred dissolution of quartz grains with a certain lattice orientation during garnet growing reaction. It is assumed in Fig. 6 that quartz grains with their *c*-axis at a high angle to the migrating phase boundary are preferably dissolved. Then it is expected that each growth sector of a garnet porphyroblast will incorporate quartz grains with their *c*-axis at a low angle to the sweeping phase boundary and that *c*-axis of quartz inclusions will show a spatial or sectorial distribution depending on the orientation of the sweeping phase boundary. However the AVA diagram (Fig. 5) does not show a domanial quartz *c*-axis fabric. Still, this possibility may not be ruled out simply based on the absence of domanial distribution of *c*-axes, because the migrating velocity of a phase boundary is known to be dependent of the lattice orientation of neighboring phases incorporated (Gleiter, 1969). Furthermore, if we consider a three-dimensional situation where each lattice plane of quartz grains has a different dissolution rate during garnet growing reaction, the entrapment process and the resulting *c*-axis fabric of quartz inclusions will be complicated and this should be explored further in the future.

Finally, it is well known that the degree of the pressure solution of quartz grains depends on their crystallographic orientation with respect to the shortening axis (e.g. Hicks et al., 1986; Tullis, 1989; Hippertt, 1994; Becker, 1995; Den Brok, 1996; Takeshita and Hara, 1998). Becker (1995) and Den Brok (1996) suggested that quartz grains with *c*-axis at a small angle from the shortening direction exhibit the least amount of pressure solution. In contrast, Hicks et al. (1986), Tullis (1989) and Hippertt (1994) suggested that both dissolution and growth parallel to *c*-axis of quartz grains are faster than other directions. If so, *c*-axis fabric parallel to the extension direction can be induced by a selective removal of quartz grains with *c*-axis subparallel to the shortening direction associated with precipitation and growth with *c*-axis parallel to the extension direction (Tullis, 1989; Hippertt, 1994; Takeshita and Hara, 1998). The role of pressure solution in developing *c*-axis fabric parallel to the lineation is difficult to identify in our samples because most of the quartz inclusions are monocrystals and because grain boundaries of polycrystalline inclusions of quartz with signatures of pressure solution should have been modified due to a thermal effect during the subsequent Barrovian-type regional metamorphism producing intertectonic garnet porphyroblasts. Interestingly, Hippertt (1994) has reported the *c*-axis fabric similar to ours (single girdle at a high angle to foliation with a sub-maximum parallel to elongation lineation) from natural phyllonite. Hippertt (1994) interpreted this as intracrystalline deformation and pressure solution playing an essential role in developing the single-girdle fabric and a sub-maximum of *c*-axis parallel to elongation lineation, respectively.

In summary, the *c*-axis fabric of quartz inclusions within intertectonic garnet porphyroblasts from the Jingok unit of the southern Imjingang belt might result from intracrystalline deformation possibly together with pressure solution prior to the garnet growth. Alternatively, the lattice preferred orientation of quartz inclusions might be produced by the selective entrapment of quartz grains with a certain lattice orientation during the growth of garnet porphyroblasts. If the lattice preferred orientation of quartz inclusions within porphyroblasts is induced by dislocation creep prior to the entrapment, our study suggests that even slip systems, dynamic recovery processes and temperature condition of deformation earlier than porphyroblast growth may be unraveled.

Acknowledgements

This work was supported by Korea Research Foundation Grant (KRF-99-042-D00138). We thank J. Ahn for informing us of the existence of plagioclase inclusions within the garnets and Y.I. Lee for allowing us to use the cathodoluminescence microscope. Detailed and constructive reviews by C.W. Passchier and an anonymous reviewer helped to improve the manuscript and are greatly appreciated.

References

Ahn, J., 1999. Regional metamorphism of pelitic schists in the Yeoncheon area, Imjingang Belt, Korea: application of cathodoluminescence. M.S. thesis, Seoul National University.

Becker, A., 1995. Quartz pressure solution: influence of crystallographic orientation. Journal of Structural Geology 17, 1395–1405.

Behr, H.J., 1980. Polyphase shear zones in the granulite belts along the margins of the Bohemian Massif. Journal of Structural Geology 2, 249–254.

Bell, T.H., Hickey, K.A., 1997. Distribution of pre-folding linear indicators of movement direction around the Spring Hill Synform, Vermont: significance for mechanism of folding in this portion of the Appalachians. Tectonophysics 274, 275–294.

Bloss, F.D., Gibbs, G.V., 1963. Cleavage in quartz. American Mineralogist 48, 821–838.

Blumenfeld, P., Mainprice, D., Bouchez, J.L., 1986. *c*-Slip in quartz from subsolidus deformed granite. Tectonophysics 127, 97–115.

Den Brok, B., 1996. The effect of crystallographic orientation on pressure solution in quartzite. Journal of Structural Geology 18, 859–860.

Garbutt, J.M., Teyssier, C., 1991. Prism ⟨c⟩ slip in the quartzites of the Oakhurst Mylonite Belt, California. Journal of Structural Geology 13, 657–666.

Gleiter, H., 1969. Theory of grain boundary migration rate. Acta Metallurgica 17, 853–862.

Hayward, N., 1990. Determination of early fold axis orientations in multiply deformed rocks using porphyroblast inclusion trails. Tectonophysics 179, 353–369.

Hicks, B.D., Applin, K.R., Houseknecht, D.W., 1986. Crystallographic influences on intergranular pressure solution in a quartzose sandstone. Journal of Sedimentary Petrology 56, 784–787.

Hippertt, J.F.M., 1993. "V"-pull-apart microstructures: a new shear-sense indicator. Journal of Structural Geology 15, 1393–1403.

Hippertt, J.F.M., 1994. Microstructures and *c*-axis indicative of quartz dissolution in sheared quartzites and phyllonites. Tectonophysics 229, 141–163.

Hsü, K.J., Li, J., Chen, H., Wang, Q., Sun, S., Sengör, A.M.C., 1990. Tectonics of south China: key to understanding West Pacific. Tectonophysics 183, 9–39.

Jiang, D., Williams, P.F., 1998. High-strain zones: a unified model. Journal of Structural Geology 20, 1105–1120.

Johnson, S.E., 1993. Unraveling the spirals: a serial thin-section study and three-dimensional computer-aided reconstruction of spiral-shaped inclusion trails in garnet porphyroblasts. Journal of Metamorphic Geology 11, 621–634.

Jung, W.S., Ree, J.-H., Park, Y., 1999. Non-rotation of garnet porphyroblasts and 3-D inclusion trail data: an example from the Imjingang belt, South Korea. Tectonophysics 307, 381–395.

Knipe, R.J., Law, R.D., 1987. The influence of crystallographic orientation and grain boundary migration on microstructural and textural evolution in an *S–C* mylonite. Tectonophysics 135, 155–169.

Law, R.D., 1990. Crystallographic fabrics: a selective review of their applications to research in structural geology. In: Knipe, R.J., Rutter, E.H. (Eds.). Deformation Mechanisms, Rheology and Tectonics. , pp. 335–352 Geological Society of London Special Publication 54.

Lister, G.S., Hobbs, B.E., 1980. The simulation of fabric development during plastic deformation and its application to quartzites: the influence of deformation history. Journal of Structural Geology 2, 355–370.

Lister, G.S., Dornsiepen, U.F., 1982. Fabric transitions in the Saxony granulite terrain. Journal of Structural Geology 4, 81–92.

MacCready, T., 1996. Misalignment of quartz *c*-axis fabrics and lineations due to oblique final strain increments in the Ruby Mountains core complex, Nevada. Journal of Structural Geology 18, 765–776.

Mainprice, D., Bouchez, J.L., Blumenfeld, P., Tubia, J.M., 1986. Dominant *c* slip in naturally deformed quartz: implications for dramatic plastic softening at high temperature. Geology 14, 819–822.

Mancktelow, N., 1995. Stereoplot Version 3. Geologisches Institut, ETH-Zentrum, Zurich.

Passchier, C.W., 1998. Monoclinic model shear zones. Journal of Structural Geology 20, 1121–1137.

Passchier, C.W., Trouw, R.A.J., 1996. Microtectonics. Springer-Verlag, Berlin.

Ree, J.-H., Cho, M., Kwon, S.-T., Nakamura, E., 1996. Possible eastward extension of Chinese collision belt in South Korea: the Imjingang belt. Geology 24, 1071–1074.

Schmid, S.M., Casey, M., 1986. Complete fabric analysis of some commonly observed quartz *c*-axis patterns. In: Hobbs, B.E., Heard, H.C. (Eds.). Mineral and Rock Deformation: Laboratory Studies — The Paterson Volume. American Geophysical Union, pp. 263–286 Geophysical Monograph 36.

Stallard, A., Shelley, D., 1995. Quartz *c*-axes parallel to stretching directions in very low-grade metamorphic rocks. Tectonophysics 249, 31–40.

Steinhardt, C.K., 1989. Lack of porphyroblast rotation in non-coaxially deformed schists from Petral Cove, South Australia and its implications. Tectonophysics 158, 127–140.

Takeshita, T., Hara, I., 1998. *c*-Axis fabrics and microstructures in a recrystallized quartz vein deformed under fluid-rich greenschist conditions. Journal of Structural Geology 20, 417–431.

Tullis, T.E., 1989. Development of preferred orientation due to anisotropic dissolution/growth rates during solution transfer creep. EOS, Transactions of the American Geophysical Unio 70 (15), 457.

Vissers, R.L.M., 1989. Asymmetric quartz *c*-axis fabrics and flow vorticity: a study using rotated garnets. Journal of Structural Geology 11, 231–244.

Yamaguchi, T., 1951. On the so-called Yonchon System and its regional metamorphism. Geological Society of Japan Journal 57, 419–438 (in Japanese with English abstract).